Transient Radiation from Pistons in an Infinite Planar Baffle

Peter R. Stepanishen

Citation: The Journal of the Acoustical Society of America **49**, 1629 (1971); doi: 10.1121/1.1912541
View online: https://doi.org/10.1121/1.1912541
View Table of Contents: https://asa.scitation.org/toc/jas/49/5B
Published by the Acoustical Society of America

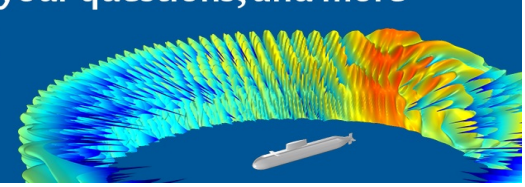

Received 24 February 1970 13.11t; 5.18

Transient Radiation from Pistons in an Infinite Planar Baffle *

PETER R. STEPANISHEN

General Dynamics/Electric Boat Division, Groton, Connecticut 06340

An approach is presented to compute the near- and farfield transient radiation resulting from a specified velocity motion of a piston or array of pistons in a rigid infinite baffle. The approach, which is based on a Green's function development, utilizes a transformation of coordinates to simplify the evaluation of the resultant surface integrals. A simple expression is developed for an impulse response function, which is the time-dependent velocity potential at a spatial point resulting from an impulse velocity of a piston of any shape. The time-dependent velocity potential and pressure for any piston velocity motion may then be computed by a convolution of the piston velocity with the appropriate impulse response. The response of an array may be computed using superposition. Several examples illustrating the usefulness of the approach are presented. The farfield time-dependent radiation from a rectangular piston is discussed for both continuous and pulsed velocity conditions. For a pulsed velocity of time duration T it is shown that the pressure at several of the field points can consist of *two* separate pulses of the same duration, when T is less than the travel time across the piston.

INTRODUCTION

The area of acoustic transient radiation phenomena has undergone considerable recent investigation. Previous investigators have considered several transient problems of interest and have obtained solutions to the appropriate boundary value problems consisting of the time-dependent wave equation with initial and boundary value conditions. Among these problems of interest, the transient acoustic loading on a baffled piston[1,2] and on a baffled strip[3] have been investigated using Laplace and Fourier transform techniques. In addition, the study of transient acoustic pressures generated by impulsively accelerated three-dimensional bodies has recently been investigated.[4]

The present paper studies the transient acoustic radiation resulting from the velocity of a piston mounted in a rigid infinite planar baffle. An excellent review of contributions in the area of transient radiation from baffled pistons has been published by Hanish.[5] A more recent survey of the literature of acoustic transients has been published by Freedman.[6] In addition, a recent paper by Freedman[7] discusses the transient radiation from radiators on plane or gently curved surfaces.

Although the necessary integral solutions to compute the transient acoustic pressures resulting from the velocities of baffled pistons have been known[5] for a considerable period of time, little effort has been devoted to obtaining numerical results. A simple approach to evaluate the Green's function integral solution for the time-dependent pressure resulting from the time-dependent velocity of a baffled piston is thus developed in the present paper and is used to obtain several numerical results. The development of the approach is based on the Green's function solution to the time-dependent boundary value problem. An impulse response function is defined which is the time-dependent velocity potential at a spatial point resulting from an impulsive velocity motion of a piston. The impulse response function, which is expressed as a surface integral, is then evaluated using a transformation from the source to observer coordinates. As a result of the transformation, a simple expression is obtained for the impulse response as a function of the spatial coordinates and time for any shape of piston radiator.

The approach is applicable to study the transient and steady-state radiation characteristics of a piston radiator or an array of pistons vibrating with a specified spatial and temporal velocity distribution where the piston velocities may be either sinusoidal or nonsinusoidal pulsed motions. Also, the approach is applicable

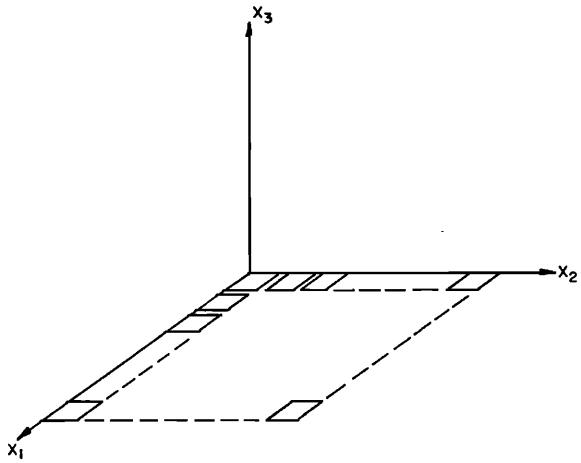

FIG. 1. A two-dimensional multielement planar array.

to the analysis of pressures at spatial points in the near- and farfield of the pistons.

I. THEORY

Consider the problem of determining the time-dependent pressure in the half-space $x_3 \geq 0$ resulting from the velocity of the piston as shown in Fig. 1. The piston is assumed to vibrate with a specified velocity which may be nonsinusoidal and/or pulsed, and the medium in the half-space is assumed to be isotropic with a constant velocity of propagation. In addition, the piston is assumed to be mounted in an infinite planar baffle, the $x_3=0$ plane, whose normal velocity is zero.

The problem of computing the pressure is readily formulated as a classical boundary value problem in terms of the velocity potential, $\phi(\mathbf{x},t)$. Using a Green's function approach, the following equation[8] is easily obtained:

$$\phi(\mathbf{x},t)=\int_0^t dt_0 \int_\sigma dS v(\mathbf{x}_0,t_0) g(\mathbf{x},t|\mathbf{x}_0,t_0), \tag{1}$$

where $v(\mathbf{x},t)$ is the piston velocity, σ is the piston area, and $g(\mathbf{x},t|\mathbf{x}_0,t_0)$ is the Green's function for the problem. It is noted that the field is specified to be initially undisturbed, i.e., the initial conditions are zero. The pressure, $p(\mathbf{x},t)$, may then be obtained from the velocity potential using the following relationship:

$$p(\mathbf{x},t)=\rho(\partial/\partial t)\phi(\mathbf{x},t), \tag{2}$$

where ρ is the density of the medium.

The integral solution for $\phi(\mathbf{x},t)$ presented in Eq. 1 can be further simplified when the piston velocity is uniform over the piston face. Assuming a uniform piston velocity $v(t)$, Eq. 1 may then be expressed as

$$\phi(\mathbf{x},t)=\int_0^t dt_0 v(t_0) \int_\sigma dS g(\mathbf{x},t|\mathbf{x}_0,t_0). \tag{3}$$

Since the Green's function for the problem is well known, i.e.,

$$g(\mathbf{x},t|\mathbf{x}_0,t_0)=\frac{1}{2\pi}\frac{\delta(t-t_0-|\mathbf{x}-\mathbf{x}_0|/c)}{|\mathbf{x}-\mathbf{x}_0|}, \tag{4}$$

where c is the velocity of propagation within the medium,[8] then $\phi(\mathbf{x},t)$ can be expressed as

$$\phi(\mathbf{x},t)=\int_0^t dt_0 v(t_0) \int_\sigma dS \frac{\delta(t-t_0-|\mathbf{x}-\mathbf{x}_0|/c)}{2\pi|\mathbf{x}-\mathbf{x}_0|}. \tag{5}$$

If Eq. 5 is first integrated over time, Rayleigh's formula[9] for the time-dependent velocity potential is easily obtained:

$$\phi(\mathbf{x},t)=\frac{1}{2\pi}\int_\sigma dS \frac{v(t-|\mathbf{x}-\mathbf{x}_0|/c)}{|\mathbf{x}-\mathbf{x}_0|}. \tag{6}$$

Alternately, Eq. 5 may be evaluated by first performing the indicated spatial integration. The velocity potential may then be expressed as a convolution integral

$$\phi(\mathbf{x},t)=v(t)*h(\mathbf{x},t), \tag{7}$$

where the asterisk is used to denote the convolution operation and $h(\mathbf{x},t)$ is defined as

$$h(\mathbf{x},t)=\int_\sigma dS \frac{\delta(t-|\mathbf{x}-\mathbf{x}_0|/c)}{2\pi|\mathbf{x}-\mathbf{x}_0|}. \tag{8}$$

The function $h(\mathbf{x},t)$ is henceforth defined as the impulse response function of the piston to the spatial point of interest, since it is easily seen from Eq. 7 that $h(\mathbf{x},t)$ is the time-dependent velocity potential at $\mathbf{x}$ resulting from an impulsive velocity of the piston.

A knowledge of the impulse response function enables the pressure to be determined upon specification of the piston velocity. The study of the impulse response function is now performed by means of a coordinate transformation to simplify the computation of the surface integral expressed in Eq. 8.

Consider the piston and geometrical variables shown in Fig. 2(a). The piston which is located in the $x_3=0$ plane may be any shape and the spatial point of interest is indicated by $\mathbf{x}$ in the figure. Locating a spherical coordinate system at the spatial point of interest, the transformation

$$R=|\mathbf{x}-\mathbf{x}_0| \tag{9}$$

is noted where R may be considered as the radius of a sphere centered at $\mathbf{x}$. Also indicated in the figure is the arc length of intersection, $L(R)$, of the piston with the surface of a sphere of radius R centered at $\mathbf{x}$. The angle $\theta(R)$ indicated in the figure is defined by points on the arc length of intersection, $L(R)$, and the normal to the $x_3=0$ plane passing through the spatial point of interest. It is further noted that $\theta(R)$ is a constant for all

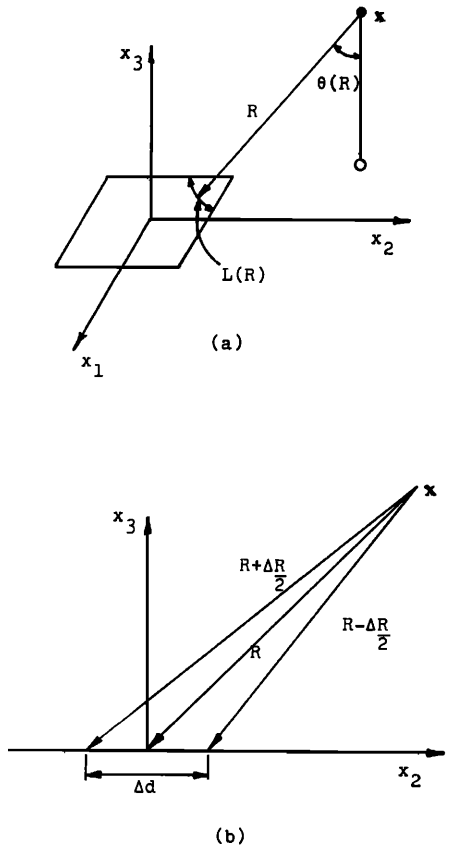

FIG. 2. Geometrical variables used in computing the impulse response.

points on $L(R)$; however, both $\theta(R)$ and $L(R)$ vary as R varies.

To simplify the evaluation of $h(\mathbf{x},t)$, the transformation in Eq. 9 is applied to Eq. 8. Since a relationship exists between the incremental surface area ΔS in the $x_3=0$ plane and R, the surface integral may be simplified. In Fig. 2(b), Δd is shown as the width of the incremental surface element in the $x_3=0$ plane resulting from the two radii, $R-\Delta R/2$ and $R+\Delta R/2$. From geometric considerations, Δd may be expressed as

$$\Delta d=\Delta R/\sin\theta(R). \tag{10}$$

Since the incremental surface area ΔS is equal to

$$\Delta S=L(R)\Delta d,$$

then, utilizing Eq. 10, ΔS may be expressed as

$$\Delta S=L(R)\Delta R/\sin\theta(R). \tag{11}$$

Taking the limit as $\Delta R\rightarrow 0$ in Eq. 11 and utilizing the transformation in Eq. 9, Eq. 8 may be expressed as

$$h(\mathbf{x},t)=\int_0^\infty \frac{\delta(t-R/c)}{2\pi R\sin\theta(R)}L(R)dR. \tag{12}$$

Making the substitution, $\tau=R/c$,

$$h(\mathbf{x},t)=\int_0^\infty \frac{\delta(t-\tau)L(c\tau)}{2\pi\tau\sin\theta(c\tau)}d\tau. \tag{13}$$

Now, using the sifting property of the δ function, Eq. 13 reduces to

$$h(\mathbf{x},t)=L(ct)/2\pi t\sin\theta(ct). \tag{14}$$

From the geometry of Fig. 2, we note $h(\mathbf{x},t)$ is a time-limited function. The function is zero until the time corresponding to the minimum radius, $R_{\min}$, of the sphere which intersects the piston and also zero after the time corresponding to the maximum radius, $R_{\max}$, of intersection. The time duration of $h(\mathbf{x},t)$ is, therefore, $(R_{\max}-R_{\min})/c$, which is larger for spatial points in the $x_3=0$ plane and smaller for points approaching the x_3 axis in the farfield of the piston. It is easily seen that the time duration of $h(\mathbf{x},t)$ is thus a function of the piston dimensions and location of the spatial point of interest, and that the maximum time duration of $h(\mathbf{x},t)$ to any point in the field is the maximum propagation time across the face of the piston.

The evaluation of $h(\mathbf{x},t)$ has been reduced from evaluating the surface integral of Eq. 8 to evaluating the simple expression in Eq. 14. It is again noted that $h(\mathbf{x},t)$ as expressed in Eq. 14 has been derived for a general spatial point with no approximation or distinction being made between near- and farfield points and is thus valid for both near- and farfield studies. Section II illustrates the application of the technique to compute pressures at both near- and far-field spatial points.

II. NUMERICAL EXAMPLES

To illustrate the application of the impulse response approach to study the transient acoustic radiation from pistons, the radiation from a circular piston shown in Fig. 3 is initially discussed. Although Morse[10] has previously obtained a solution for the velocity potential

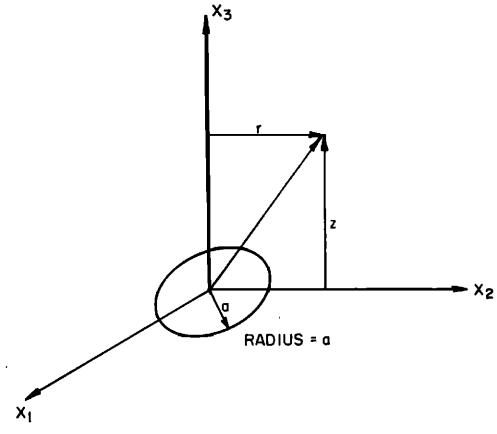

FIG. 3. Circular piston in a planar baffle.

and pressure in the field resulting from an impulsive velocity of the piston, the solution is valid only in the farfield. Morse utilized a time domain approach which is quite similar to the impulse response approach being described here and may be obtained from the expression for the impulse response by specifying the arc lengths of intersections (see Eq. 14) to be straight lines.

To solve for the transient radiation from a circular piston for both near- and farfield points, the curvature of the arc lengths of intersection as shown in Fig. 2 must be accounted for. After a little geometrical manipulation, the impulse response $h(\mathbf{x},t)$ may be evaluated for the two cases of $a>r$ and $a\leq r$ using the geometry of Fig. 3. For the case $a>r$,

$$\begin{aligned} h(\mathbf{x},t)&=0, \quad ct<z,\\ &=c, \quad z<ct<R',\\ &=\frac{c}{\pi}\cos^{-1}\left\{\frac{(ct)^2-z^2+r^2-a^2}{2r[(ct)^2-z^2]^{\frac{1}{2}}}\right\}, \quad R'<ct<R,\\ &=0, \quad ct>R, \end{aligned} \tag{15}$$

where $R'=[z^2+(a-r)^2]^{\frac{1}{2}}$, $R=[z^2+a(+r)^2]^{\frac{1}{2}}$. It is noted that R' and R are the shortest and longest distances, respectively, from the observation point to the circumference of the piston. For the case $a<r$, we obtain

$$\begin{aligned} h(\mathbf{x},t)&=0, \quad ct<R',\\ &=\frac{c}{\pi}\cos^{-1}\left\{\frac{(ct)^2-z^2+r^2-a^2}{2r[(ct)^2-z^2]^{\frac{1}{2}}}\right\}, \quad R'<ct<R,\\ &=0, \quad ct>R, \end{aligned} \tag{16}$$

where R' and R are defined above. The expressions for $h(\mathbf{x},t)$ are identical to earlier results published by Oberhettinger.[11] Oberhettinger's analysis of the problem was performed using integral transforms and is thus complementary to the impulse response analysis of the problem.

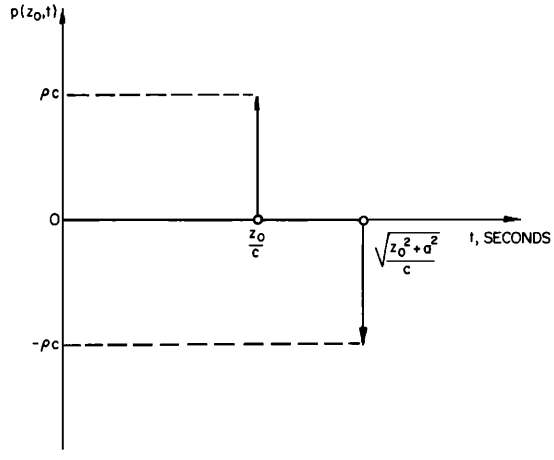

FIG. 4. On-axis pressure resulting from an impulsive velocity motion of a circular piston.

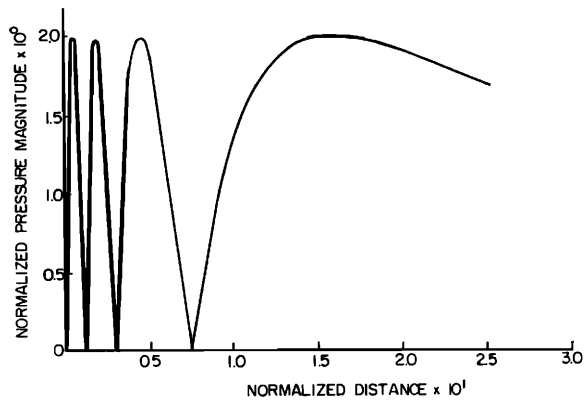

FIG. 5. On-axis pressure magnitude for a circular piston of radius $a=4\lambda$.

The impulse response of the circular piston to an on-axis point is now discussed in more detail. Using Eq. 15, it is easily seen that $h(\mathbf{x},t)$ is a delayed rectangular pulse with a time duration of $[(z_0^2+a^2)^{\frac{1}{2}}-z_0]/c$, where z_0 is the distance of the spatial point above the piston. To obtain the on-axis pressure resulting from an impulse velocity motion, Eqs. 2 and 15 are used. The pressure versus time is shown in Fig. 4 and may be expressed as follows:

$$p(z_0,t)=\rho c\left\{\delta\left[t-\frac{z_0}{c}\right]-\delta\left[t-\frac{(z_0^2+a^2)^{\frac{1}{2}}}{c}\right]\right\}, \tag{17}$$

where $\delta[\cdots]$ is the Dirac delta function.

The pressure at an on-axis point is thus seen to consist of two Dirac delta or impulse functions of opposite strength equal to the characteristic impedance of the medium. The time delay of the initial impulse corresponds to the propagation time from the center of the piston to the spatial point, and the time delay of the second impulse corresponds to the propagation time from the edge of the piston to the spatial point.

Several interesting numerical results are easily obtained from Eq. 17. Initially, we consider the field point at $z_0=0$ and a piston of infinite radius. From Eq. 17 and the use of the sifting property of the Dirac delta function, it can be shown that the pressure and particle velocity at $z_0=0$ are related by the familiar relationship

$$p=\rho cv, \tag{18}$$

where v is the velocity of the x_1-x_2 plane. Since the vibration of the piston of infinite radius is equivalent to the vibration of an infinite plane, the particle velocity and pressure must be related by the familiar plane-wave relationship shown in Eq. 18. Although the case $z_0=0$ has been discussed, the case $z_0\neq 0$ could be easily analyzed following a similar analysis.

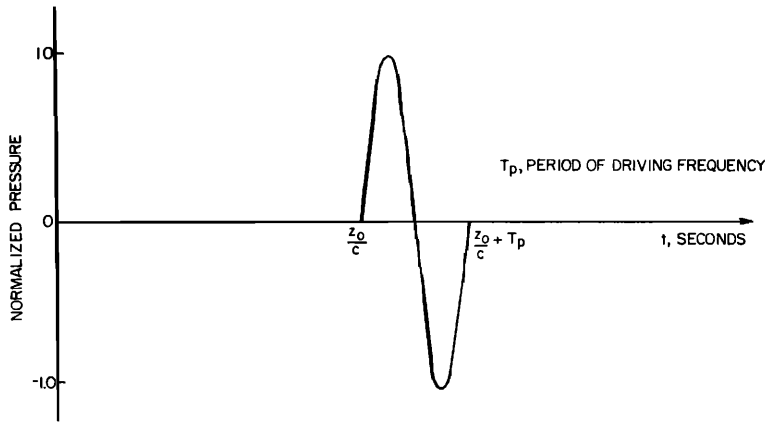

FIG. 6. Normalized nearfield on-axis pressure at a minima.

The on-axis pressure resulting from the sinusoidal velocity of a piston of finite radius is now discussed. A transfer function $G(z_0,s)$ is now defined as follows:

$$G(z_0,s)=\mathcal{L}\{p(z_0,t)\}, \tag{19}$$

where $\mathcal{L}\{\cdots\}$ denotes the Laplace transform of the indicated function in brackets and s is the transform complex variable. Since $p(z_0,t)$ is the pressure at z_0 resulting from an impulsive velocity of the piston, then $G(z_0,s)$ is the transfer function relating the on-axis pressure to a sinusoidal piston velocity.

For the general case $z_0\neq 0$, it is easily shown that $G(z_0,s)$ may be expressed as

$$G(z_0,s)=2\rho c\exp\frac{-(z_0^2+a^2)^{\frac{1}{2}}s}{c}\times\sinh\left\{\left[\frac{(z_0^2+a^2)^{\frac{1}{2}}-z_0}{c}\right]s\right\}. \tag{20}$$

Studying $G(z_0,s)$ as a function of z_0/λ, the curve shown in Fig. 5 is obtained by evaluating Eq. 20 at a fixed frequency, where $a=4\lambda$. The curve shows the nearfield oscillations of the normalized on-axis pressure magnitude resulting from a sinusoidal piston velocity, i.e., $|G(z_0,s)|/\rho c$, and illustrates the region of spherical spreading. Kinsler and Frey[12] present an identical curve which was derived directly from the steady-state field equations for the case $a=4\lambda$.

Although the steady-state on-axis pressure has been obtained using the impulse response approach, the main emphasis in the present paper is the investigation of transient phenomena. Of particular interest is the time-dependent behavior of the pressure at the maximum and minimum locations shown in Fig. 5. The velocity of the circular piston is thus initially specified to be a sinusoidal function turned on at $t=0$ and vibrating at a frequency such as $a=4\lambda$.

The time-dependent pressures at the on-axis field points are easily obtained using the impulse response approach. Figure 6 presents the normalized pressure, $p(z_0,t)/\rho c$, at the minimum location $z_0/\lambda=7.5$ shown in Fig. 5. The transient pressure exists for a single cycle, and the steady-state condition of zero pressure is then reached. The time-dependent pressure at the maximum location $z_0/\lambda=5.0$ is shown in Fig. 7. It is noted from Fig. 7 that the transient pressure exists for one and a half cycles and the peak transient pressure is less than the steady-state pressure of the pressure maxima. It is thus noted that the large transient pressures are associated with small steady-state pressures. These results are in general agreement with studies conducted by Sherman[13] on the transient pressures generated from arrays of circular pistons.

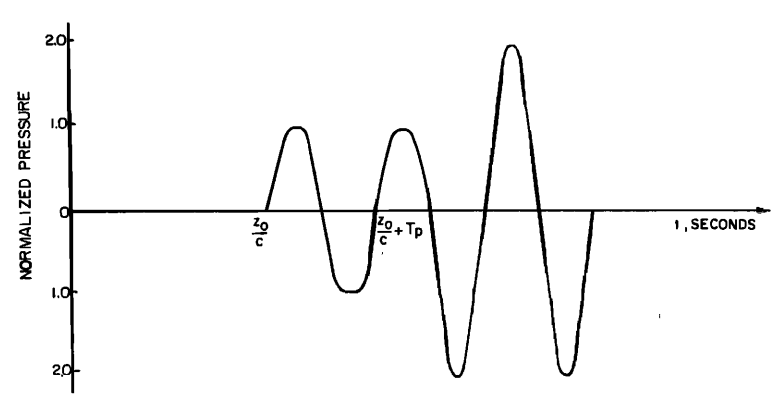

FIG. 7. Normalized nearfield on-axis pressure at a maxima.

The minima and maxima of the on-axis pressure are easily explained in terms of the impulse response approach. The minima occur at spatial points where the time interval between the impulse functions shown in Fig. 4 is an integer number of periods of the driving frequency. For the pressure maxima, the time interval is an odd multiple of half-periods of the drive frequency. An alternate, but equivalent, explanation is that the maxima or minima occur where the difference in path length from the edge and center of the piston to the spatial point is an even or odd multiple of half-wavelengths.

For the preceding cases the nearfield on-axis pressures were investigated for a velocity which was specified to be a sinusoidal function of infinite time duration after turn on. We now consider the case where the piston velocity is a specified pulse with a finite time duration after turn on, and we also discuss the pressure at points in the near- and farfield of the piston. Freedman, in an earlier paper,[7] has discussed the farfield radiated pressure for this case. It is again noted that the on-axis pressures are initially discussed, since several interesting transient phenomena occur at the on-axis field points.

Since Eq. 17 expresses the on-axis pressure resulting from an impulsive piston velocity, the pressure from any specified piston velocity $v(t)$ is simply the convolution of $v(t)$ with the indicated function in Eq. 17. Performing the convolution and noting the sifting property of the delta function, the pressure at z_0 is easily expressed as follows:

$$p(z_0,t)=\rho c\left\{v\left(t-\frac{z_0}{c}\right)H(t-z_0/c)-v\left[t-\frac{(z_0^2+a^2)^{\frac{1}{2}}}{c}\right]H\left[t-\frac{(z_0^2+a^2)^{\frac{1}{2}}}{c}\right]\right\}, \quad (21)$$

where $H[\cdots]$ is the familiar Heaviside function, i.e.,

$$H(t)=1, \quad t>0,$$
$$=0, \quad t<0.$$

It is easily seen from Eq. 21 that the pressure is composed of an initial pulse and a delayed pulse, both with the same time history as the piston velocity. If the pulse duration of the piston velocity is less than the time delay between the pulses, two separate pressure pulses are observed at the spatial point. Apart from the change of sign of the second pulse, the time history of the pulses is identical to the piston pulse. If the time duration of the piston velocity is greater than the time delay between the pulses, only a single pressure pulse, which is the sum of the two overlapping pulses, is observed. The pressures in Figs. 6 and 7 are now easily noted to be special examples of the preceding case, where the delayed pulse of infinite time duration adds in phase or out of phase with the original sinusoidal function to obtain the pressure maxima or minima.

The preceding discussion has been limited to a study of the pressure at on-axis points in the nearfield of the circular piston. To study the pressure at an arbitrary near- or farfield point, the general expression for the impulse response which is indicated in Eqs. 15 or 16 must be substituted into Eq. 7 and the resultant velocity potential substituted into Eq. 2. The use of Eqs. 15 or 16 is dependent upon whether the r coordinate of the field point is less than or greater than the piston radius (see Fig. 3). A simple expression may now be derived relating the pressure and piston velocity by utilizing Eqs. 2 and 7 with the appropriate impulse response. Performing the indicated substitutions and differentiation, it is readily shown that the pressure may be evaluated from the following expression:

$$p(\mathbf{x},t)=\rho\int_{-\infty}^{\infty}\dot{h}(\mathbf{x},t-\tau)v(\tau)d\tau, \quad (22)$$

where $\dot{h}(\mathbf{x},t)$ is the time derivative of the impulse response, and $\dot{h}(\mathbf{x},t)$ may contain Dirac delta functions corresponding to discontinuities in $h(\mathbf{x},t)$.

Several properties of the radiated field from a circular piston can be deduced from Eq. 22. If $h(\mathbf{x},t)$ exhibits discontinuities, Eq. 22 clearly indicates that the resultant pressure would contain components of pressure which are delayed and weighted replicas of the piston velocity. The discontinuities in $h(\mathbf{x},t)$ would thus yield the "replica pulses" discussed in Freedman's work.[7] Since $h(\mathbf{x},t)$ is, in general, a continuous function, the "replica pulses" would not be observed in the radiated field of a circular piston. It is, however, noted that for spatial points, where $r<a$, discontinuities in $h(\mathbf{x},t)$ do occur, and replica pulses would thus result for short pulse durations as shown earlier for on-axis points. It is also noted that for points where $r>a$, infinite discontinuities of opposite sign occur at the beginning and end of $\dot{h}(\mathbf{x},t)$, although $h(\mathbf{x},t)$ is a continuous function. The occurrence of these discontinuities can be shown by differentiating Eq. 16. Morse[8] has also noted the infinite discontinuities in the farfield pressures resulting from an impulsive velocity of the circular piston, i.e., $\dot{h}(\mathbf{x},t)$. Unlike the on-axis points where Dirac delta functions in $\dot{h}(\mathbf{x},t)$ (see Fig. 4) result in replica pulses, replica pulses will not occur for points where $r>a$, since $\dot{h}(\mathbf{x},t)$ is a continuous function with infinite discontinuities at its endpoints.

It can, however, be noted from Eq. 22 that the infinite discontinuities at the endpoints of $\dot{h}(\mathbf{x},t)$ yield large contributions to the field pressures. Unlike Freedman's results,[7] which assume that the discontinuities yield the only contribution to the pressure, the impulse response approach yields the exact time-dependent pressures. When the time duration of the piston velocity is small relative to the time duration of $h(\mathbf{x},t)$, the present approach shows the pressures to be amplitude-distorted time-expanded versions of the piston velocity pulse.

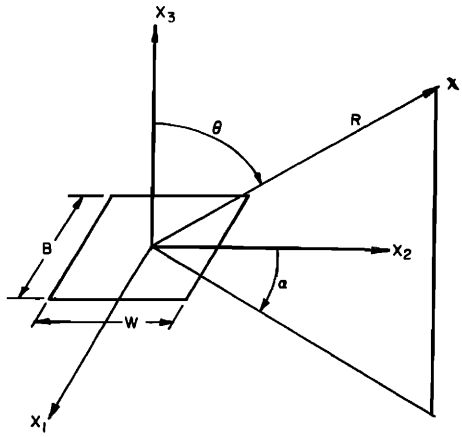

FIG. 8. Rectangular piston in a planar baffle.

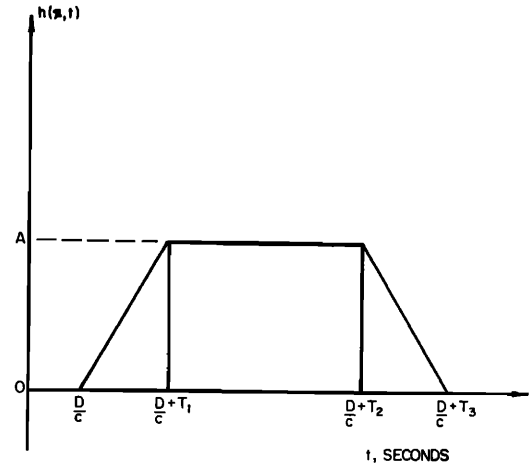

FIG. 9. Farfield impulse response from a rectangular piston. $A=Bc/2\pi R\cos\alpha\sin\theta$; $T_1=(B/c)\sin\alpha\sin\theta$; $T_2=(W/c)\cos\alpha\sin\theta$; $T_3=(B\sin\alpha+W\cos\alpha)\sin\theta/c$; and D equals minimum distance from x to the piston.

Thus, unlike the replica pulses presented by Freedman,[7] the pressures are distorted pulses of the original piston velocity where the amount of distortion is dependent on the piston velocity and the field point of interest.

The near- and farfield radiation characteristics of a square or rectangular piston shown in Fig. 8 can also be determined using the impulse response approach. The application of the approach to study farfield pressures is now presented. For points where $R\gg W$ and $R\gg B$, the impulse response in Eq. 14 can be simply evaluated using approximations resulting from the inequalities. The arc lengths of intersection (see Fig. 2) required to compute $h(\mathbf{x},t)$ are approximately straight lines. In addition, $\theta(ct)$ (see Fig. 2) is approximately constant in value and the $1/t$ variation in Eq. 14 can be approximated as $1/(R/c)$. The impulse response to a farfield point can then be simply computed and is shown in Fig. 9.

Once again the steady-state radiation characteristics may be obtained from the impulse response. Transforming $h(\mathbf{x},t)$ and using the pressure-velocity potential relation, the pressure transfer function may be expressed as

$$G(\mathbf{x},s)=\rho\frac{WB}{2\pi R}e^{-(Rs/c)}\left\{\frac{\sinh[(B/2c)\sin\alpha\sin\theta s]}{(B/2c)\sin\alpha\sin\theta s}\right\}\times\left\{\frac{\sinh[(W/2c)\cos\alpha\sin\theta s]}{(W/2c)\cos\alpha\sin\theta s}\right\}. \quad (23)$$

Substituting $s=j\omega$ into the above equation, the classical steady-state result for the beam pattern is obtained.

Several time-dependent pressures at spatial points in the farfield of the rectangular piston shown in Fig. 8 are now presented. The points are specified to lie on a hemispherical surface of radius R, and the pressures are presented at several spatial points defined by the angles shown in Fig. 8.

For all the pressures shown in the following figures the piston velocity was assumed to be a pulsed sinusoid with a time duration equal to three periods of the carrier frequency and the pressures are normalized to the peak on-axis pressure. The piston length, B, is also conveniently normalized by the carrier wavelength λ, and was specified as $B/\lambda=6.0$. It is thus noted that the pulse duration of the piston velocity is equal to one-half the travel time over the piston length.

The time-dependent pressure at $\alpha=90°$ and $\theta=4°$ resulting from the pulsed velocity is shown in Fig. 10. The transient portion of the pressure waveform consists of the first and last one-half cycle of data, and the remaining pressure is the steady-state part of the pressure which may be obtained from Eq. 21. Figure 11 presents the time-dependent pressure at the spatial point defined by $\alpha=90°$ and $\theta=14°$. The transient portion of the waveform consists of the initial and last one and a half cycles of data. Although the velocity exists for only

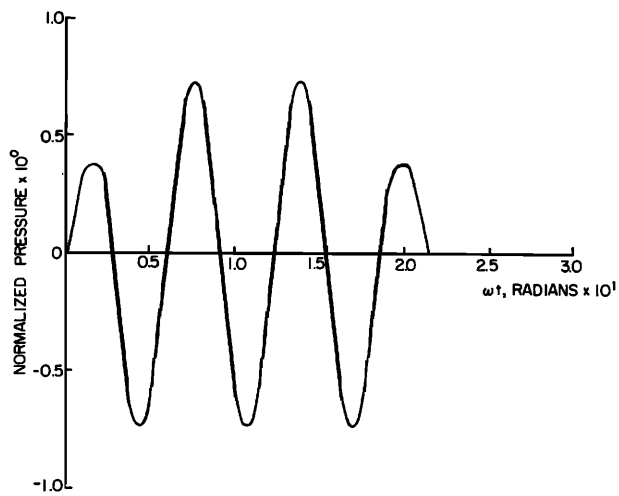

FIG. 10. Normalized pressure at $\theta=4°$.

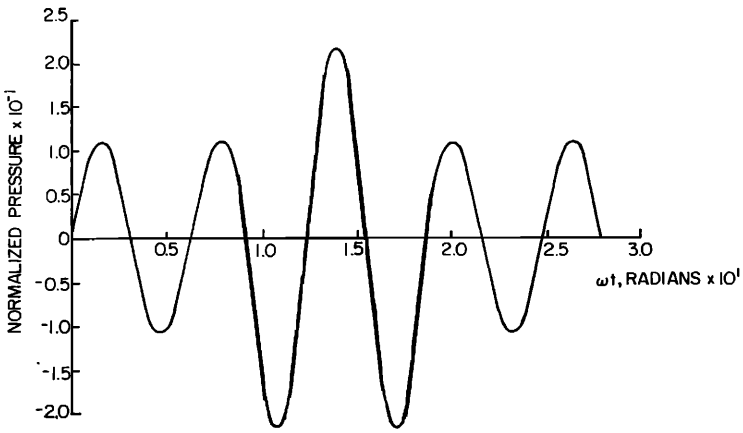

FIG. 11. Normalized pressure at $\theta=14°$.

three periods of the carrier frequency, the pressure is noted to exist for 4.5 cycles of data. Figure 12 presents the pressure at $\theta=30°$ and $\alpha=90°$. The steady-state pressure computed from Eq. 21 is zero; thus the entire time history of the pressure is a transient, and a steady-state condition is never reached. The time duration of the pressure is again noted to be larger than the time duration of the piston velocity. Figure 13 presents the pressure at $\alpha=90°$ and $\theta=41.5°$. The steady-state portion of the pressure is again zero; however, the pressure consists of two pressure-transient pulses separated by a zero pressure condition.

The pressures that are shown in the figures indicate several interesting transient phenomena. These transient effects become increasingly significant as the ratio of the pulselength to travel time over the piston decreases. When the pulselength becomes less than the travel time across the piston, the field pressures may radically differ from the piston velocity as shown in the preceding figures. Also, under the same conditions the pressure at field points greater than a critical angle from the normal to the piston will consist of two separate pulses as indicated in Fig. 13. In all cases it is noted that, although the velocity input exists for only three cycles of the carrier frequency, the field pressure exists over a longer time duration which is the result of the propagation effect over the length of the piston. As $\theta \rightarrow 90°$, the time duration of the pressure transient thus approaches nine periods of the carrier frequency.

An additional point of interest is noted from the time integral of the pressure at each point. The integral of each pressure in Figs. 10–13 is zero and is thus in agreement with a general rule credited to Stokes by Rayleigh[9] stating that the time integral of the pressure at a spatial point is zero for an outgoing wave disturbance.

The preceding figures have shown that the farfield time-dependent pressures can differ considerably from the velocity of the piston. Although the farfield on-axis pressure is proportional to the piston acceleration, the off-axis pressures are related to the piston velocity by Eq. 2 and the convolution integral in Eq. 7. The pressure and piston velocity can also be directly related using the convolution integral expression in Eq. 22. Utilizing the impulse response shown in Fig. 7, $\dot{h}(\mathbf{x},t)$ can be easily shown to consist of two Dirac delta functions of equal and opposite weight with different time delays at the spatial points of interest indicated in Figs. 10–13. The delta functions are again the result of discontinuities in $\dot{h}(\mathbf{x},t)$ which are associated with the piston edges. These discontinuities yield two replica pulses of pressure in the field, and the pressures in Figs. 10–12 are easily explained in terms of the overlapping pulses. In Fig. 13 the pulses do not overlap in time, and the two separate pulses, which appear to originate at the piston edges perpendicular to the plane of interest, are observed.

Although the impulse response approach has been used to obtain farfield pressures, again it is noted that

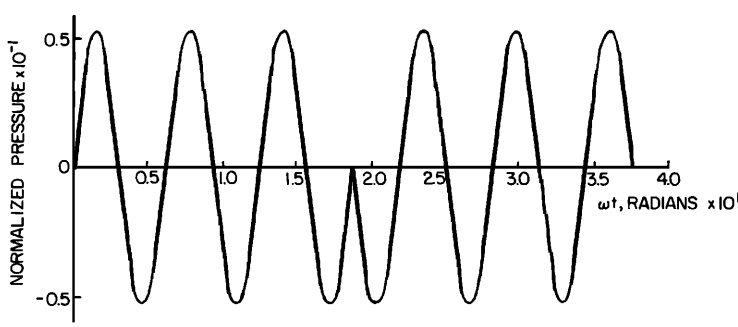

FIG. 12. Normalized pressure at $\theta=30°$.

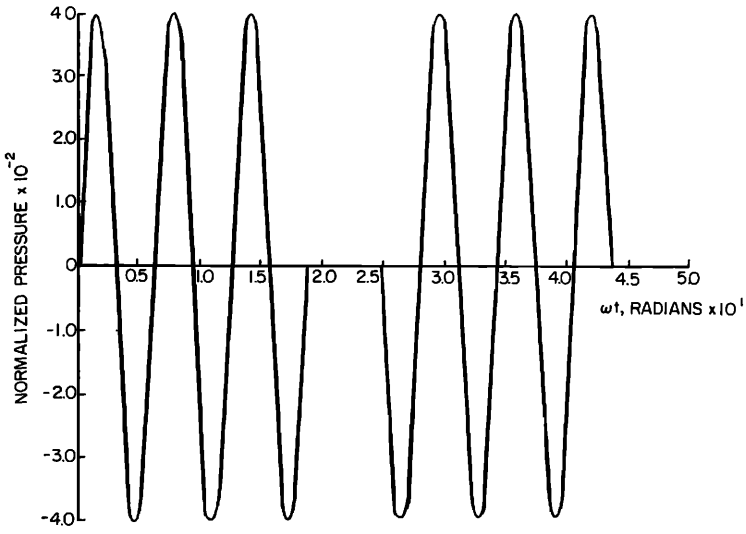

FIG. 13. Normalized pressure at $\theta=41.4°$.

the approach is also valid for nearfield calculations. Unlike the circular piston, the impulse response to a general field point for a rectangular piston cannot, however, be evaluated in a simple closed form. To evaluate nearfield pressures it is, therefore, necessary to evaluate numerically $h(\mathbf{x},t)$ at the spatial point of interest. The pressure can then be evaluated utilizing Eqs. 2 and 7. Since $h(\mathbf{x},t)$ is again a continuous function for points not directly above or on the piston, the replica pulses will not be observed in the nearfield pressures. For points directly above or on the piston, the initial discontinuity in $h(\mathbf{x},t)$ will, however, yield a single replica pulse contribution to the total pressure at the spatial point.

III. CONCLUSIONS

An approach has been developed and presented to compute both near- and farfield transient radiation from a piston or array of pistons mounted in an infinite planar rigid baffle. Although the general solution of the problem as a surface integral (see Eq. 3) has been well known, little if any effort has been expended in obtaining numerical results. The present paper sets forth a simple method of evaluating the surface integral and thus the time-dependent pressure resulting from the specified velocity of any bandwidth for a piston or array of pistons.

It is noted that for certain piston shapes and field point locations, closed form solutions for the pressures can be obtained using the approach. A simple expression was derived to compute the time-dependent pressure at any point in the medium resulting from the specified velocity of a circular piston, and the time-dependent characteristics of the radiated field were then discussed. In addition, the farfield pressures resulting from the pulsed velocity of a rectangular piston were presented and discussed. In either of the principal planes of the rectangular piston, the pressure at a spatial point was shown to consist of two pulses with a time history identical to that of the piston velocity. Several time-dependent pressures were presented illustrating transient pressure phenomena resulting from over-lapping of the pulses. Finally, it was shown that for a piston velocity with a time duration less than the travel time over the piston, the two separate pressure pulses can be observed in regions of the field.

The approach that was developed in the present paper to compute time-dependent pressures formed the basis for the work that was presented in earlier papers[14,15] by the author. It is noted that the first paper was concerned with the development of an approach to compute time-dependent interaction forces among pistons in planar arrays. In the second paper an approach was developed to compute the time-dependent force on a piston as a result of its specified velocity. The present paper is thus the third in a series of papers discussing transient acoustic phenomena related to pistons mounted in planar baffles.

* A portion of this paper was presented at the 79th meeting of the Acoustical Society on 22 April 1970, at Atlantic City, New Jersey [J. Acoust. Soc. Amer. 48, 101(A) (1970)] and also formed part of the author's doctoral thesis at Pennsylvania State Univ., December 1969.

[1] J. W. Miles, "Transient Loading of a Baffled Piston," J. Acoust. Soc. Amer. 25, 200–203 (1953).

[2] V. Mangulis, "The Time-Dependent Force on a Sound Radiator Immediately Following Switch-On," Acustica 17, 223–227 (1966).

[3] J. W. Miles, "Transient Loading of a Baffled Strip," J. Acoust. Soc. Amer. 25, 204–205 (1953).

[4] M. C. Junger and W. C. Thompson, "Oscillatory Acoustic Transients Radiated by Impulsively Accelerated Bodies," J. Acoust. Soc. Amer. 38, 978–986 (1965).

[5] S. Hanish, "A Review of World Contributions from 1945 to 1965 to the Theory Radiation, Chapter III, Theory of Transient Radiation," Naval Res. Lab. Mem. Rep. 1688 (10 Mar. 1966).

[6] A. Freedman, "Transient Fields of Acoustic Radiators," J. Acoust. Soc. Amer. **48**, 135–138 (1970).
[7] A. Freedman, "Sound Field of Plane or Gently Curved Pulsed Radiators," J. Acoust. Soc. Amer. **48**, 221–227 (1970).
[8] P. M. Morse and K. U. Ingard, *Theoretical Acoustics* (McGraw–Hill, New York, 1968), p. 369.
[9] J. W. Strutt Lord Rayleigh, *Theory of Sound* (Dover, New York, 1945), Vol. 2, Chap. 14.
[10] P. M. Morse, *Vibration and Sound* (McGraw–Hill, New York, 1948), p. 346.
[11] F. Oberhettinger, "On Transient Solutions of the Baffled Piston Problem," J. Res. Nat. Bur. Stand. **65B**, 1–6 (1961).
[12] L. E. Kinsler and A. R. Frey, *Fundamentals of Acoustics* (Wiley, New York, 1962), p. 177.
[13] C. H. Sherman and D. A. Moran, "Transient Sound Field of Simple Arrays of Planar Pistons," Parke Mathematical Lab. Rep. No. 1 (Nov. 1966).
[14] P. R. Stepanishen, "An Approach to Compute Time-Dependent Interaction Forces and Mutual Radiation Impedances between Pistons in a Rigid Infinite Baffle," J. Acoust. Soc. Amer. **49**, 283–293 (1971).
[15] P. R. Stepanishen, "The Time-Dependent Force and Radiation Impedance on a Piston in a Rigid Infinite Planar Baffle," J. Acoust. Soc. Amer. **49**, 841–849 (1971).